Route to Chaos and Unified Dynamical Framework of Multi-Species Ecosystems

R. Delabays[1] and Ph. Jacquod[1,2,3]
[1] *School of Engineering, University of Applied Sciences of Western Switzerland HES-SO, CH-1950 Sion, Switzerland*
[2] *Andlinger Center for Energy and the Environment, Princeton University, Princeton, NJ 08544 USA*
[3] *Department of Quantum Matter Physics, University of Geneva, CH-1211 Geneva, Switzerland*
(Dated: March 20, 2025)

We investigate species-rich mathematical models of ecosystems. Much of the existing literature focuses on the properties of equilibrium fixed points, in particular their stability and feasibility. Here we emphasize the emergence of limit cycles following Hopf bifurcations tuned by the variability of interspecies interaction. As the variability increases, and owing to the large dimensionality of the system, limit cycles typically acquire a growing spectrum of frequencies. This often leads to the appearance of strange attractors, with a chaotic dynamics of species abundances characterized by a positive Lyapunov exponent. We find that limit cycles and strange attractors preserve biodiversity as they maintain dynamical stability without species extinction. We give numerical evidences that this route to chaos dominates in ecosystems with strong enough interactions and where predator-prey behavior dominates over competition and mutualism. Based on arguments from random matrix theory, we further conjecture that this scenario is generic in ecosystems with large number of species, and identify the key parameters driving it. Overall, our work proposes a unifying framework, where a wide range of population dynamics emerge from a single model.

Introduction. One of the main challenges in theoretical ecology is to connect predictions from mathematical models of population dynamics to empirical observations of species coexistence in natural or laboratory-controlled ecosystems [1]. It is established that individual populations fluctuate in time, often with large qualitative and quantitative differences between species [2–5]. In some instances, population abundances exhibit synchronized, periodic oscillations, while in others population dynamics appears chaotic [6–13]. It is highly desirable to find out whether the wide range of observed dynamics can be captured by varying few parameters of a unifying mathematical model, and if yes, what are the key characteristics this model should retain. Investigating mathematical models can furthermore shed light on fundamental qualitative questions such as whether populations fluctuations are endogenous or exogenous, i.e., if they are generated by intrinsic interactions or by external sources [7, 14].

In this letter, we numerically investigate large Lotka-Volterra models with random interactions, which are standard multi-species models of population dynamics. We emphasize the richness of their dynamics as a function of two key parameters which are (i) the variability σ in interspecies interactions, and (ii) the off-diagonal covariance parameter γ of the interaction matrix. Our main finding is that, for sufficiently large ratio of predator-prey pairs of species, the stable fixed-points prevailing at weak interaction variability generically lose their stability through Hopf bifurcations. Limit cycles emerge, where surviving species have periodically oscillating abundances. At still stronger interactions, strange attractors appear, possibly from cascades of bifurcations, which lead to a chaotic dynamics of population abundances characterized by a positive largest Lyapunov exponent. This route to chaos illustrates how stationarity, oscillating periodicity and chaos in the dynamics of species abundances exist in rather general models of population dynamics, depending on σ and γ. One important result is that all observed population dynamics in multi-species ecosystems can be reproduced by a unified mathematical model.

Much of theoretical ecology is based on the surmise that the observed states and dynamics of ecosystems can be described by the time-asymptotic behavior of mathematical models. Accordingly, there has been a significant focus on the equilibrium fixed points of large systems of competing species, their stability and feasibility [15–22] One key parameter is the variability σ of the interspecies interaction. It has been found that a unique, asymptotically stable fixed point exists at weak enough $\sigma < \sigma_c$ [15, 17, 21, 22], and that σ_c increases in ecosystems with dominating predator-prey interactions [18, 19]. For $\sigma > \sigma_c$, one enters a phase with multiple unstable equilibria [22]. Stabilization may still occur via species extinction, which drives the ecosystem to a novel, stable fixed point with reduced biodiversity. Beyond fixed points, the emergence of limit cycles through Hopf bifurcation has been emphasized, albeit for small systems with only few species [23–27]. Further regimes with aperiodic persistent dynamics have recently been highlighted at stronger interactions and/or larger number of species [28], in ecosystems with sparse interactions [29, 30] or communities with migrations [31]. In contrast to this mainstream philosophy focusing on the time-asymptotic behavior of mathematical models, several works have advocated that sufficiently large ecosystems have long relaxation times so that, by nature, they are in a transient state [32–35]. Such large relaxation times may follow from the slowing down of the dynamics in ecosystems close to criticality [36, 37]. Below we

show that all these different behaviors naturally emerge in different regimes of a single mathematical model, as a function of only two parameters.

Model and method. Population dynamics in multi-species ecosystems is commonly studied in the framework of the generalized Lotka-Volterra model [38]

$$\dot{N}_i = N_i \left[\kappa_i - N_i - \frac{\mu}{S} \sum_{j=1}^{S} N_j - \frac{\sigma}{\sqrt{S}} \sum_{j=1}^{S} \mathbb{A}_{ij} N_j \right] . \quad (1)$$

Eq. (1) determines the time-evolution of the normalized abundance $N_i(t) \geq 0$ of species $i = 1, 2, \dots S$, as a function of its intrinsic growth rate κ_i and its interaction with other species. Interactions have a finite average μ and a variability σ. Fluctuations in interaction strengths between pairs of species are encoded in the components $\mathbb{A}_{ij}$ of the interaction matrix $\mathbb{A}$. Being interested in large, heterogeneous ecosystems with no particular structure, we follow a random matrix theory (RMT) approach [15, 39, 40] and take $\mathbb{A}_{ij}$ to be normally distributed with vanishing average and covariances given by

$$\langle \mathbb{A}_{ij} \mathbb{A}_{kl} \rangle = \delta_{ik}\delta_{jl} + \gamma \delta_{il}\delta_{jk} . \quad (2)$$

The off-diagonal covariance parameter $\gamma \in [-1, 1]$ tunes from competitive or mutualistic pairs of species ($\gamma = 1$; where the spectrum of $\mathbb{A}$ is real) to only predator-prey pairs of species ($\gamma = -1$; ; where the spectrum is purely imaginary) [41]. For $\gamma = 0$, $\mathbb{A}$ belongs to the Ginibre ensemble or random matrices [42].

The generalized Lotka-Volterra model of Eq. (1) assumes that $N_i(t)$ is real and varies continuously. This is a legitimate assumption only as long as $N_i(t)$ is sufficiently large. Large fluctuations have been observed in numerical simulations of Eq. (1), where some species resurrect from minuscule abundances, effectively corresponding to extinction. As a matter of fact, the dynamics of Eq. (1) leads to species extinction only for asymptotically long times, and the standard procedure to solve this *atto-fox* problem [43] is to introduce a small, but finite extinction threshold N_c. When $N_i(t_c) < N_c$, extinction occurs and $N_i(t > t_c) \equiv 0$. We will set $N_c = 10^{-20}$ but have checked that other choices lead to the same conclusions as presented below. Our focus is on the parameters σ and γ defining the variability of the interspecies interactions and accordingly we fix the growth rates, the initial number of species and the average interaction at values $\kappa_i \equiv 1$, $S = 157$ and $\mu = 5$. We have checked that varying μ does not change our conclusions as long as $\mu > 0$.

The RMT approach to ecosystem dynamics dates back at least to May's seminal work [15]. Fixed-points $\vec{N}^*$ of Eq. (1) are defined by $\dot{N}_i^* = 0$ and the dynamics in their vicinity is governed by the stability matrix $\mathbb{M}$

$$\delta\dot{\vec{N}} = \mathbb{M}\, \delta\vec{N} , \quad (3a)$$

$$\mathbb{M}_{ij} = -N_i^* (\delta_{ij} + \mu/S + \sigma \mathbb{A}_{ij}/\sqrt{S}) . \quad (3b)$$

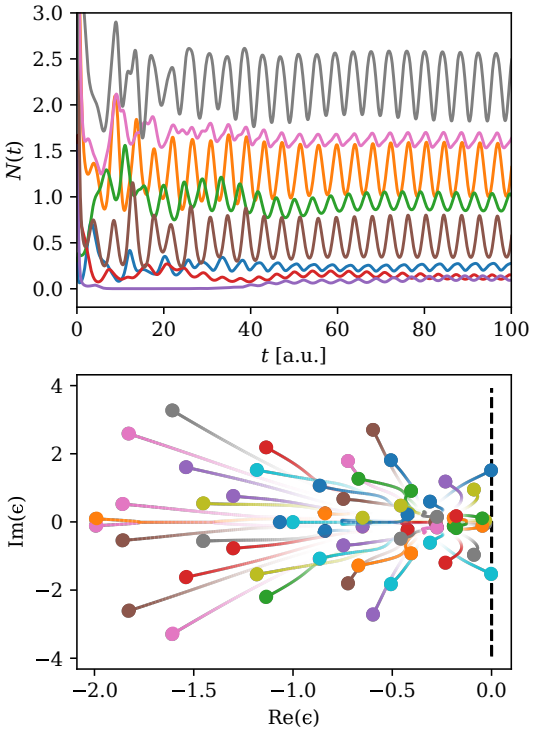

Figure 1. Top: abundances for 8 of the $N_s = 61$ surviving species oscillating in a limit cycle for a realization of the model of Eq. (1), with $\sigma = 4.05$ and $\gamma = -0.5$. Bottom: Evolution of the eigenvalues of the stability matrix $\mathbb{M}$ for $\sigma \in [0, 4.02]$ (more faded colors indicate smaller values of σ). Stability of the fixed point is lost when a pair of complex-conjugated eigenvalues cross the imaginary axis, resulting in a Hopf bifurcation and the emergence of the limit cycle shown in the top panel.

The fixed-point is stable as long as the spectrum of $\mathbb{M}$ lies entirely in the left half of the complex plane. The average density of eigenvalues of $\mathbb{A}$ is distributed within a zero-centred ellipse in the complex plane with semi-axes $\sigma(1+\gamma)$ [$\sigma(1-\gamma)$] in the real [imaginary] direction [44]. The ellipse is shifted to the left by the identity matrix [the Kronecker symbol in Eq. (3b)], while the constant μ-term in Eq. (3b) adds an outlier eigenvalue $-\mu$ [21]. Assuming an homogeneous distribution of populations, $N_i^* \simeq N_0 = \mathcal{O}(1)$, the fixed-point is parametrically stable for $\sigma < (1+\gamma)^{-1}$. Beyond that border, fixed-point stability may be recovered via species extinctions, $N_i^* \to 0$, except for a number $N_s < S$ of surviving species, because then, the stability matrix $\mathbb{A}^{(r)}$ is reduced by removing rows and lines from $\mathbb{A}$, corresponding to the extinct species. Then, the spectrum of $\mathbb{A}^{(r)}$ has an elliptic support with semi-axes $\sigma(1 \pm \gamma)\sqrt{N_s/S}$. Stability then bounds the number of surviving species $N_s/S \leq [\sigma(1+\gamma)]^{-2}$. Note that this argument says nothing about the bifurcation through which fixed-points lose stability.

Results. For $\gamma \neq 1$ the eigenvalues of the real, asymmetric matrix $\mathbb{M}$ are either real, or come in complex-conjugated pairs. This opens up the possibility that the fixed-point loses its stability through a Hopf bifurcation,

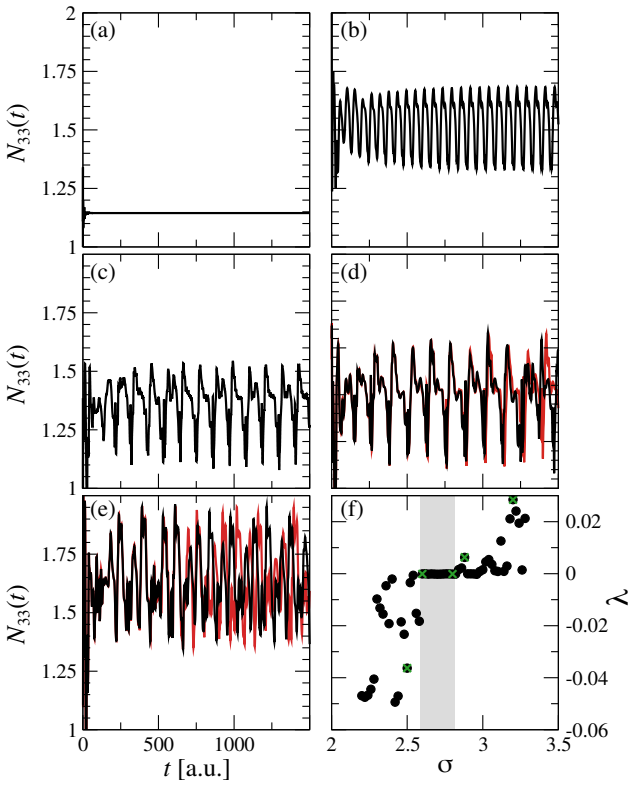

Figure 2. Emergence of a limit cycle and transition to chaos for the model of Eq. (1), with $\gamma = -0.5$. The time-evolution of the species abundance N_{33} is plotted for (a) $\sigma = 2.5$, (b) $\sigma = 2.6$, (c) $\sigma = 2.8$, (d) $\sigma = 2.85$, and (e) $\sigma = 3.19$. Panel (f) shows the numerically computed largest Lyapunov exponent λ, with green crosses corresponding to the cases shown in panels (a-e). In panel (d) and (e), two initially nearby sets of abundances diverge from one another (black and red curves), reflecting the corresponding positive λ. Different trajectories repeat similar patterns, albeit in different sequences and without periodicity. Together with $\lambda > 0$, this is characteristic of the presence of a strange attractor. There is no such sensitivity to initial conditions in the three other cases, where $\lambda < 0$ when the dynamics is attracted to a fixed point [as in panel (a)], and $\lambda = 0$ (grey area) in the presence of a limit cycle [as in panels (b) and (c)].

after which the ecosystem dynamics is attracted to a stable limit cycle. Such a Hopf bifurcation is illustrated in Fig. 1, where the top panel shows periodic oscillations in abundances of the surviving species which are related in the bottom panel to the crossing of the imaginary axis by a complex-conjugated pair of eigenvalues. For large random matrices with $\gamma = 0$ it has been shown that only $\mathcal{O}(\sqrt{S})$ of the S eigenvalues are real [45–47], which suggests that such Hopf bifurcations are the rule rather than the exception in ecosystems with high biodiversity.

Directly following the bifurcation, cycles exhibit sinusoidal oscillations with a single frequency, determined by the imaginary part of the pair of involved eigenvalues. More harmonics emerge as σ increases further, until the cycle disappears. Cycle disapearance can happen because the cycle loses either its stability – for instance through an inverse Hopf bifurcation – or its feasibility – for instance because one or several species reach the extinction threshold N_c somewhere along the cycle. The dynamics of a single-species as σ passes through and keeps increasing beyond a Hopf bifurcation is shown in Fig. 2. It illustrates a third mechanism by which a periodic cycle turns into a strange attractor. To quantify this transition to chaos, we numerically calculated the largest Lyapunov exponent λ [48]. As expected, $\lambda < 0$ in the fixed-point regime, $\sigma \lesssim 2.59$. Following the Hopf bifurcation, $\lambda = 0$ as long as the limit cycle remains stable [panels (b) and (c)], which corresponds to the dynamics in the direction tangential to the cycle. Upon further increase of σ, $\lambda > 0$ as one enters the chaotic regime, with a population dynamics governed by a strange attractor. The black and red trajectories in panels (d) and (e) illustrate the associated sensitivity to initial conditions, where population trajectories repeat similar-looking patterns, albeit at irregular time intervals and following sequences depending strongly on initial conditions. We stress that the abrupt fluctuations exhibited by λ in both the fixed-point and the strange attractor regimes reflect fast dynamical changes with σ. Numerical error bars in panel (f) of Fig. 2 are smaller than symbol sizes, in particular, $|\lambda| \lesssim 10^{-5}$ in the limit cycle regime $2.59 \lesssim \lambda \lesssim 2.82$ (grey area in Fig. 2).

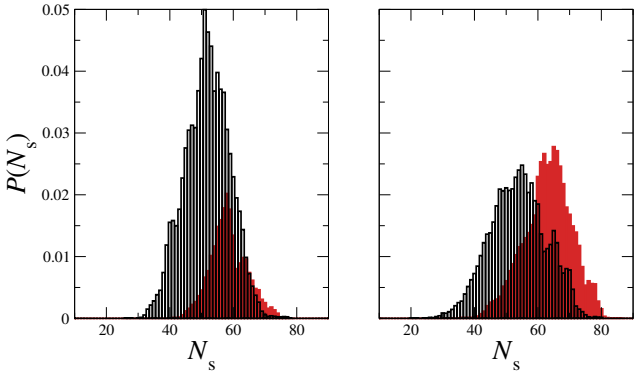

Figure 3. Distribution of the number of surviving species for the model of Eq. (1), with $\sigma = 2$, $\gamma = 0$ (left) and $\sigma = 4$, $\gamma = -0.5$ (right). Black histograms correspond to fixed point solutions and red histograms to limit cycle solutions. Distributions are calculated over 400 realizations of the interaction matrix $\mathbb{A}_{ij}$, each with 25 different initial abundances. In all considered cases, the system converges to either a fixed point or a limit cycle. Distributions correspond to 22.5% (left panel) and 47.6 % of cycles (right panel).

The occurence of Hopf bifurcations is of central importance for theoretical ecology. It extends the stability of population coexistence beyond the loss of fixed-point stability, without the need for species extinction. The resulting increasing biodiversity is illustrated in Fig. 3. It is obvious that the average number of coexisting species at fixed σ is higher for ecosystems equilibrating to limit

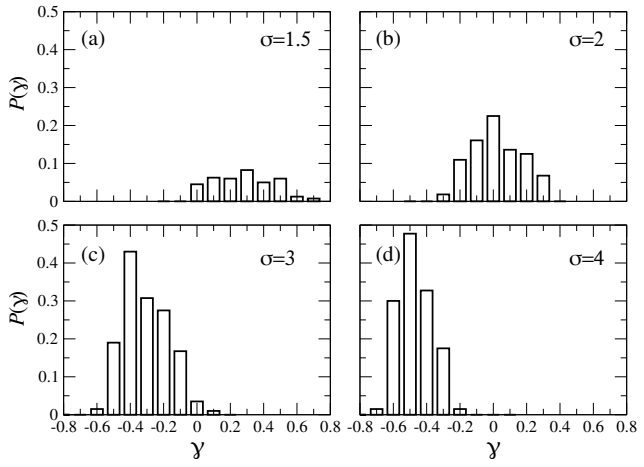

Figure 4. Probability to find the system in a state of persistent dynamics – either a limit cycle or a state of chaotic dynamics on a strange attractor – as a function of γ, and for $\sigma = 1.5$ [Panel(a)], 2 [(b)], 3 [(c)] and 4 [(d)]. Data have been calculated over ensembles of 100 different interaction matrices, each with 5 different initial conditions.

cycles ($\langle N_s \rangle = 58.4$ and 63) than to fixed-points ($\langle N_s \rangle = 51.8$ and 53.7). The prevalence of limit cycles further depends on both the variability σ of interspecies interaction and on the off-diagonal covariance parameter γ. As a matter of fact, to have a limit cycle, one needs a large enough σ to have a bifurcation in the first place. Second, the bifurcation must also involve a pair of complex-conjugated eigenvalues of the stability matrix. Both the value of σ and the probability that a complex-conjugated pair of eigenvalues triggers the bifurcation depend on γ. Fig. 3 suggests that more negative values of γ, together with the associated larger value of σ to have a bifurcation favor the occurence of limit cycles. This fact is confirmed in Fig. 4, which shows the probability $P(\gamma)$ that the ecosystem reaches a state of persistent dynamics. The numerical detection method employed for this statistical analysis does not differentiate between limit cycles and chaotic motion on a strange attractor, however sampling those data indicate that chaotic motion sets in only at larger interactions, and constitutes a significant fraction of the data only for $\sigma = 4$. Work to better quantify this fraction is currently underway. Data for larger σ are not shown as they exhibit mass extinctions, with only very few surviving species at best, except for the smallest values of γ.

The observed increased probability to find limit cycles at negative values of γ is related to the associated increased fraction of pairs of complex-conjugated eigenvalues in the spectrum of the stability matrix. Neglecting inhomogeneities in the fixed-point abundancies N_i^*, this spectrum is real for $\gamma = 1$ and purely imaginary for $\gamma = -1$, and it is expectable that the fraction of real eigenvalues decreases as γ decreases. To the best of our knowledge, the only mathematically rigorous result at intermediate values of γ is that only a fraction $\mathcal{O}(\sqrt{S})$ of the eigenvalues are real for the Ginibre ensemble, i.e., at $\gamma = 0$ [45–47]. While these observations suggest more frequent occurences of limit cycles as γ decreases, what truly matters is whether the extreme eigenvalue with largest real part is real or complex. Calculating how likely that is as a function of γ is a formidable task and we are unaware of any rigorous result in this direction. We therefore resort to numerical calculations (See Supplemental Material [49], Fig. S1). As expected, we find that the probability of a complex extreme eigenvalue increases with decreasing γ. To translate this result into a probability to have a limit cycle emerge through a Hopf bifurcation, we still need to take into account that there is no bifurcation at $\gamma = -1$, since there, increasing σ only stretches the spectrum in the imaginary direction. We therefore expect that moderately negative values of γ should favor the emergence of limit cycles. This qualitative argument is confirmed by the data shown in Fig. 4. A second numerical result shown in Fig. S1 [49] is that this probability increases with increasing number S of species.

We translate these results into the language of theoretical ecology. Noting that γ interpolates between ecosystems consisting purely of pairs of either mutualistic or competitive species for $\gamma = 1$, to ecosystems with only predator-prey pairs of species for $\gamma = -1$ [41], persistent oscillating behavior in population abundances are expected to be prevailing in large, sufficiently interacting ecosystems with a majority of predator-prey pairs.

Conclusions. It has long been known that multispecies ecosystems described by sets of coupled ordinary differential equations of the type given in Eq. (1) may exhibit any dynamical behavior [50]. Here we have emphasized a route joining the previously observed phases governed by attractive fixed-points to those exhibiting persistent dynamics. Because species in ecosystems and food webs interact with one another in a necessarily asymmetric way, fixed-point instabilities may occur via a Hopf bifurcation. The resulting limit cycles preserve biodiversity, since at least for some range of interaction variability, their stability does not necessitate species extinctions.

Models of theoretical ecology are not expected to precisely reflect ecosystem behaviors. Instead, they may shed light on different, observed behaviors of real or lab-controlled ecosystems at a statistical level. In that respect, our work emphasizes the emergence of chaotic behaviors of species population in ecosystems. Recent analysis of population time series found evidence of chaotic behavior in at least 30% of the studied populations [11]. Fig. 2 further emphasizes parametrically sizable regimes with small Lyapunov exponents, which has also been observed [7, 11]. Other regimes with strong sensitivity to even minor parametric changes [E.g. at $\sigma \gtrsim 3$ in Fig. 2(f)] are characteristic of systems close to criticality as discussed in Refs. [36, 37]. Since criticality slows down

the dynamics, the behavior of ecosystems in this latter regime is transient by nature and not governed by any long-time asymptotic. That ecosystems are governed by transient behaviors has been postulated in Refs. [28, 32–35]. The emergence of Hopf bifurcations at negative values of γ finally explains recent results where ecosystems with dominating predator-prey interactions display oscillatory behaviors in their population dynamics [51]. The present work illustrates that all the different, observed or theoretically postulated behaviors naturally emerge from a single, unified model, without the need for exogeneous intervention. The task at hand now is obviously to try and determine, at least qualitatively, model parameters corresponding to specifically observed ecosystems. Our work has simplified that task in that it identified the two key model parameters σ and γ driving transitions between different dynamical behaviors.

There are several important direction in which our work should be extended. Among them, we mention first, that we are currently investigating the frequency of occurence of strange attractors vs. restabilization after species extinction at large σ. Second, further investigations should extend our results to interaction matrices reflecting more realistic topologies of known ecological networks [52]. Third, investigating species distributions may give precious information on the conditions under which biodiversity and rarity may coexist [36]. Fourth, ecosystem parameters are modified by climate changes [53–55]. Investigating changes in ecosystem functioning under climate-induced changes in trophic interactions is of paramount interest. It would evidently have a strong influence on ecosystem functioning in the critical and chaotic regimes with strong parameter sensitivity. There are certainly many other interesting extensions.

Acknowledgments. We thank Christian Mazza and Xavier Richard for introducing us to theoretical ecology and population dynamics. RD was supported by the Swiss National Science Foundation, under grant nr. 200021_215336.

[1] R.M. May and A.R. McLean, Eds., *Theoretical Ecology: Principles and Applications*, Oxford University Press (2007).
[2] E. Ranta, V. Kaitala, and P. Lundberg, Oikos **83**, 376 (1998).
[3] P. Lundberg, E. Ranta, J. Ripa, and V. Kaitala, Trends in Ecology and Evolution **15**, 460 (2000).
[4] P. Inchausti and J. Halley, J. Animal Ecology **72**, 899 (2003).
[5] J. Vandermeer, BioScience **56**, 967 (2006).
[6] A. Hastings, C.L. Holm, S. Ellner, P. Turchin, H.C.J. Godfray, Annu. Rev. Ecol. Syst. **24**, 1 (1993).
[7] S. Ellner and P. Turchin, The American Naturalist **145**, 343 (1995).
[8] M.D. Hunter and P.W. Price, Ecological Entomology **23**, 216 (1998).
[9] J. Huisman and F.J. Welssing, Nature **402**, 401 (1999).
[10] E. Benincà, H. Huisman, R. Heerkloss, K.D. Jöhnk, P. Branco, E.H. Van Nes, M. Scheffer and S.P. Ellner, Nature **451**, 822 (2008).
[11] T. Rogers, B. Johnson, and S. Munch, Nat Ecol Evol **6**, 1105 (2022).
[12] J. Prendergast et al., *Global Population Dynamics Database, Knowledge Network for Biocomplexity* (2010), doi:10.5063/F1BZ63Z8.
[13] M.T. Pearce, A. Argawala, and D.S. Fisher, Proc. Natl. Acad. Sci. **117**, 14572 (2020).
[14] M. Scheffer, S. Rinaldi, J. Huisman, and F.J. Weissing, Hydrobiologia **491** 9 (2003).
[15] R.M. May, Nature **238**, 413 (1972).
[16] A. Roberts, Nature **251**, 601 (1974).
[17] H. Rieger, J. Phys. A:Math. Gen. **22**, 3447 (1989).
[18] S. Allesina and S. Tang, Nature **483**, 205 (2012).
[19] S. Tang, S. Pawar, and S. Allesina, Ecology Lett. **17**, 1094 (2014).
[20] Y.V. Fyodorov and B.A. Khoruzhenko, Proc. Natl. Acad. Sc. **113**, 6827 (2016).
[21] M. Clenet, F. Massol, and J. Najim, J. Math. Biology **87**, 13 (2023).
[22] V. Ros, F. Roy, G. Biroli, G. Bunin, and A.M. Turner, Phys. Rev. Lett. **130**, 257401 (2023).
[23] M.E. Gilpin, Am. Naturalist **109**, 51 (1975).
[24] J. Coste, J. Peyraud, and P. Coulet, SIAM J. Appl. Math. **36**, 516 (1979).
[25] L. Gardini, R. Lupini, and M.G. Messia, J. Math. Biol. **27**, 259 (1989).
[26] G.F. Fussmann, S.P. Ellner, K.W. Shertzer, and N.G. Hairston, Science **290**, 1358 (2000).
[27] E.A. McGehee, N. Schutt, D.A. Vasquez, and E.Peacock-López, Intl. J. Bif. and Chaos **18**, 2223 (2008).
[28] J. Hu, D.R. Amor, M. Barbier, G. Bunin, and J. Gore, Science **378**, 85 (2022).
[29] F. Roy, M. Barbier, G. Biroli, and G. Bunin, PLoS Comput. Biol. **16**, e1007827 (2020).
[30] S. Marcus, A.M. Turner, and G. Bunin, Phys. Rev. E **109**, 064410 (2024).
[31] I. Dalmedigos and G. Bunin, PLoS Comput. Biol. **16**, e1008189 (2020).
[32] A. Hastings and K. Higgins, Science **263**, 1133 (1994).
[33] S.J. Schreiber, Th. Pop. Biology **64**, 201 (2003).
[34] A.Yu. Morozov, M. Banerjee, and S.V. Petrovskii, J. Th. Biology **396**, 116 (2016).
[35] A. Hastings, K.C. Abbott, K. Cuddington, T. Francis, G. Gellner, Y.-C. Lai, A. Morozov, S. Petrovskii, K. Scranton, and M.L. Zeeman, Science **361**, eaat6412 (2018).
[36] R.V. Solé, D. Alonso, and A. McKane, Phil. Trans. R. Soc. Lond. B **357**, 667 (2002).
[37] T. Mora and W. Bialek, J. Stat. Phys. **144**, 268 (2011).
[38] N.S. Goel, S.C. Maitra, and E.W. Montroll, Rev. Mod. Phys. **43**, 231 (1971).
[39] S. Allesina and S. Tang, Popul. Ecol. **57**, 63 (2015).
[40] I. Akjouj, M. Barbier, M. Clenet, W. Hachem, M. Maïda, F. Massol, J. Najim, and V.C. Tran, Proc. R. Soc. A **480**, 20230284 (2024).
[41] For a simplified model with a random distribution of $\mathbb{A}_{ij} = \pm 1$, the ratio of predator-prey pairs with $\mathbb{A}_{ij} = -\mathbb{A}_{ji}$ is equal to $(1-\gamma)/2$.
[42] J. Ginibre, J. Math. Phys. **6**, 440 (1965).
[43] D. Mollison, Math. Biosciences **107**, 255 (1991).

[44] H.J. Sommers, A. Crisanti, H. Sompolinsky, and Y. Stein, Phys. Rev. Lett. **60**, 1895 (1988).
[45] A. Edelman, E. Kostlna, and M. Shub, J. Am. Math. Soc. **7**, 247 (1994).
[46] A. Edelman, J. Multivariate Analysis **60**, 203 (1997).
[47] E. Kanzieper and G. Akemann, Phys. Rev. Lett. **95**, 23021 (2005).
[48] G. Benettin, L. Galgani, A. Giorgilli, and J.-M. Strelcyn, Meccanica **15**, 9 (1980); Meccanica **15**, 21 (1980).
[49] See Supplemental Material for numerical results on extreme eigenvalues of the stability matrix and different dynamics obtained for the same interaction matrix, with different initial conditions.
[50] S. Smale, J. Math. Biol. **3**, 5 (1976).
[51] A.M. Mambuca, C. Cammarota, and I. Neri, Phys. Rev. E **105**, 014305 (2022).
[52] Y. Fried, N.M. Shnerb, and D.A. Kessler, Phys. Rev. E **96**, 012412 (2017).
[53] B.C. Rall, O. Vucic-Pestic, R.B. Ehnes, M. Emmerson, and U. Brose, Glob. Change Biol. **16**, 2145 (2010).
[54] G. Englund, G. Öhlund, C.L. Hein, and S. Diehl, Ecology Lett. **14**, 914 (2011).
[55] E.C. Parain, R.P. Rohr, S.M. Gay, and L.-F. Bersier, Am. Naturalist **193**, 227 (2019).

Route to Chaos in Complex, Multi-Species Ecosystems : Supplemental Material

EXTREME EIGENVALUE OF A REAL ASYMMETRIC RANDOM MATRIX

The occurence of a Hopf bifurcation requires that the first eigenvalue to cross the imaginary axis has a finite imaginary part – in which case one actually has a pair of different, complex-conjugated eigenvalue. Therefore, the probability of a Hopf bifurcation is larger, if the probability that the extreme eigenvalue has a finite imaginary part is larger. Fig. S1 shows this probability for the matrix $\mathbb{A}$ of Eqs. (1–2) as a function of γ and for different matrix sizes. The probability is larger at more negative values of γ, moreover, it increases with the system size. Once concludes that Hopf bifurcations are the rule rather than the exception for sufficiently large ecosystems with $\gamma < 0$.

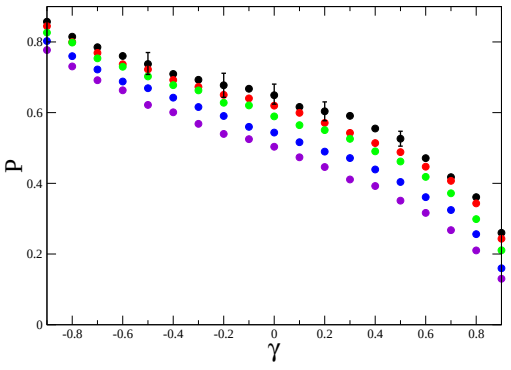

Figure S1. Probability that the eigenvalue with largest real part of a random matrix defined by Eq. (2) is imaginary, as a function of γ. Data correspond to averages over 10000 matrices of size $S = 57$ (violet), 157 (blue) and 557 (green), and 5000 matrices with $S = 1057$ (red) and 2057 (black). Note the limiting cases (not shown) $P(\gamma = -1) = 1$ and $P(\gamma = 1) = 0$.

LONG-TIME ASYMPTOTIC FOR DIFFERENT INITIAL CONDITIONS

When σ is smaller than the May bound, $\sigma < 1/(1+\gamma)$, the long-time asymptotic is a single, globally attractive fixed point. We illustrate that, at larger σ, and with a finite (though small) extinction threshold, $N_c = 10^{-20}$, different asymptotic behaviors can be reached. Fig. S2 shows five different dynamics obtained from five different initial distribution of populations subjected to the same interaction matrix $\mathbb{A}_{ij}$. For clarity, we show only five species for each case. Two initial conditions converge toward a limit cycle and three toward a fixed point. The three fixed points are evidently different. The two cycles differ mostly by the survival of species #75 in panel (a) and its extinction in panel (e). As a consequence, the oscillations are similar, but with larger amplitude in panel (e). We stress that the dynamics has been investigated for much longer times than shown, and that in all cases, the dynamics remain the same as for $t \gtrsim 350$, in particular with the same amplitudes of oscillations in panels (a) and (e).

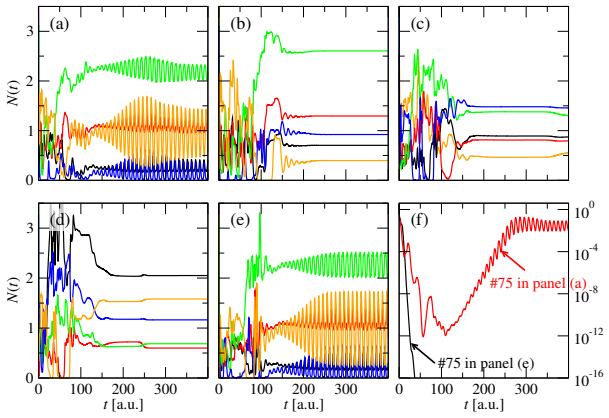

Figure S2. Panels (a-e): Five different dynamics, corresponding to the same realization of the interaction matrix, with five different initial distribution of populations. The limit cycles reached in panels (a) and (e) differ by the presence of one additional species in panel (a). Species oscillate about almost the same average values, with however large amplitude in panel (e). Panel (f): Dynamics of species #75 which persists in panel (a) but goes extinct in panel (e). Changing the extinction threshold to $N_c = 10^{-10}$ leads to two different fixed points for the initial conditions of panels (a) and (e). Five species are shown for each panel. The number of surviving species is $N_s = 57$ [panel (a)], 51 [panel (b)], 49 [panel (c)], 46 [panel (d)] and 56 [panel (e)].

Setting a higher extinction threshold $N_c = 10^{-10}$ makes species #75 disappear also in panel (a), however it further modifies the dynamics so that both the cases of panel (a) and (e) converge toward different fixed points (not shown). While the specifically followed dynamics depends on N_c, the general conclusion that different dynamics can be followed by different initial conditions is general.